Small proline-rich proteins (SPRRs) are epidermally produced antimicrobial proteins that defend the cutaneous barrier by direct bacterial membrane disruption

Chenlu Zhang[1*], Zehan Hu[2, 3], Abdul G. Lone[1], Methinee Artami[1], Marshall Edwards[1], Christos C. Zouboulis[4], Maggie Stein[1], Tamia A. Harris-Tryon[1, 2*#]

[1]Department of Dermatology, University of Texas Southwestern Medical Center, Dallas, TX, 75390
[2]Department of Immunology, University of Texas Southwestern Medical Center, Dallas, TX, 75390
[3]State Key Laboratory of Microbial Metabolism, Joint International Research Laboratory of Metabolic & Developmental Sciences, School of Life Sciences and Biotechnology, Shanghai Jiao Tong University, Shanghai, China, 200240
[4]Department of Dermatology, Venereology, Allergology and Immunology, Dessau Medical Center, Brandenburg Medical School Theodore Fontane and Faculty of Health Sciences Brandenburg, 06847 Dessau, Germany.

*Correspondence to:
tamia.harris-tryon@utsouthwestern.edu
chenlu.zhang@utsouthwestern.edu

Abstract

Human skin functions as a physical barrier, preventing the entry of foreign pathogens while also accommodating a myriad of commensal microorganisms. A key contributor to the skin landscape is the sebaceous gland. Mice devoid of sebocytes are prone to skin infection, yet our understanding of how sebocytes function in host defense is incomplete. Here we show that the small proline-rich proteins, SPRR1 and SPRR2 are bactericidal in skin. SPRR1B and SPPR2A were induced in human sebocytes by exposure to the bacterial cell wall component lipopolysaccharide (LPS). Further, LPS injected into mouse skin triggered the expression of the mouse SPRR orthologous genes, *Sprr1a* and *Sprr2a*, through stimulation of MYD88. Both mouse and human SPRR proteins displayed potent bactericidal activity against MRSA (methicillin-resistant *Staphylococcus aureus*), *Pseudomonas aeruginosa* and skin commensals. Thus, *Sprr1a*$^{-/-}$;*Sprr2a*$^{-/-}$ mice are more susceptible to MRSA and *Pseudomonas aeruginosa* skin infection. Lastly, mechanistic studies demonstrate that SPRR proteins exert their bactericidal activity through binding and disruption of the bacterial membrane. Taken together, these findings provide insight into the regulation and antimicrobial function of SPRR proteins in skin and how the skin defends the host against systemic infection.

68 **Introduction**

69 The skin is the human body's largest organ, with direct contact with the external environment
70 [1]. As a result, the skin surface continuously encounters a diverse microbial community
71 including bacteria, fungi, viruses and parasites [2–4]. When host defense is impaired, skin
72 infection results. Thus, skin and soft tissue infections pose a considerable public health threat
73 [5]. The majority of infections of the skin are caused by *Staphylococcus aureus* (*S. aureus*) [6].
74 Additionally, *Pseudomonas aeruginosa* (*P. aeruginosa*) infections in burn patients are one of
75 the most common causes of mortality [7]. Adding to the challenges of treating infections posed
76 by these pathogens has been the development of antibiotic resistant strains of bacteria such as
77 methicillin resistant *Staphylococcus aureus* (MRSA) [8].

78 Skin antimicrobial proteins (AMPs) play an essential role in defending the host from the
79 invasion of pathogens [9,10]. Mammalian antimicrobial proteins are evolutionarily ancient
80 immune effectors that rapidly kill bacteria by targeting bacterial cell wall or cell membrane
81 structures [11,12]. Several distinct antimicrobial protein families, such as β-defensins,
82 cathelicidins, resistin and S100 proteins, have been identified and characterized in skin [13,14].
83 However, we still have a limited understanding of the arsenal of antimicrobial proteins
84 expressed by the skin, the regulatory networks that control the expression of AMPs, and how
85 AMPs function to protect mammalian skin surfaces. Even less is known about the contribution
86 that skin appendages make to host defense.

87 Sebaceous glands (SGs) are specialized epithelial cells that cover the entire skin surface except
88 the palms and soles. SGs excrete a lipid-rich and waxy substance called sebum to the skin
89 surface [15–17]. SGs are believed to contribute to the antimicrobial functions of the skin [13], yet few

current studies have examined the role of SGs in skin host defense. Here we show the impact of the bacterial cell wall component lipopolysaccharide (LPS) on human sebocytes and demonstrate that bacterial lipoproteins stimulate the expression of members of the small proline-rich protein (SPRR) family. SPRR proteins were originally identified as markers of terminal differentiation and function as substrates of transglutaminase in the crosslinked cornified envelope present at the skin surface [18,19]. In this study, we demonstrate that SPRR proteins function as antimicrobial proteins. *Sprr1a*$^{-/-}$;*Sprr2a*$^{-/-}$ mice are more susceptible to MRSA and *P. aeruginosa* skin infection, revealing that SPRR proteins protects against pathogenic bacterial infections of the skin. We also show mechanistically that the bactericidal activity of SPRR proteins is mediated through the binding and disruption of bacterial membranes. Taken together our findings support a novel antimicrobial function of SPRR proteins in skin.

Results

SPRR proteins are induced by LPS in human sebocytes

As a first step towards understanding the role of the sebaceous gland in skin host defense, we performed whole transcriptome RNA-sequencing to compare transcript abundances in human immortalized sebaceous gland cells (SZ95) treated with lipopolysaccharide (LPS) to untreated sebocytes (Fig 1A). LPS, a lipoprotein which coats the surface of Gram-negative bacteria, had broad impacts on gene expression in human sebocytes, including the increased expression of inflammatory cytokines, chemokines and antimicrobial proteins (Fig 1A). Notably, three members of the small proline rich family of proteins (SPRR) were markedly upregulated in

113 sebocytes after LPS treatment (Fig 1A). To confirm that the expression of SPRR genes were
114 induced by LPS, we used quantitative reverse transcription PCR (qRT-PCR) to analyze the
115 change of the human *SPRR1B, SPRR2A, SPRR2D* transcript abundance in SZ95 cells.
116 Consistent with our RNA-seq results, LPS-treated SZ95 cells displayed significant increase in
117 the relative expression of *SPRR* family genes compared to vehicle treated cells (Fig 1B).
118 Additionally, dose response and time course experiments revealed that 1μg LPS treatment for
119 16 hours is optimal for induction of *SPRR* family genes expression (fig S1). Consistent with
120 the qRT-PCR results, SPRR proteins expression also increased after LPS treatment in SZ95
121 cells (Fig 1C, 1D). LPS is a pattern associated molecular pattern (PAMP) known to trigger gene
122 transcription through the pattern recognition receptor, Toll-like receptor (TLR) 4 [20]. We
123 therefore tested a panel of PAMPs to see if other foreign stimuli would trigger the expression
124 of the *SPRR* genes in human sebocytes. Interestingly, two other lipoproteins, Pam3CSK4 and
125 FSL-1, stimulate the expression of *SPRR1B*, *SPRR2A,* and *SPRR2D* genes in human sebocytes
126 (fig S2), indicating that sebocytes respond to bacterial lipoproteins by expressing SPRR1 and
127 SPRR2 proteins.
128 Next, we decided to further explore whether heat-inactivated bacteria could induce the
129 expression of SPRR genes in sebocytes. We used qRT-PCR to analyze the change of the human
130 *SPRR2A* transcript abundance in SZ95 cells after various heat-inactivated bacteria treatment.
131 Interestingly, only the Gram-negative bacteria tested could trigger SPRR2A expression (fig
132 S3). Taken together, these data establish that bacterial lipoproteins triggers the expression of
133 *SPRR* genes in human sebocytes.

134

135 **SPRR proteins are upregulated by the injection of LPS in mouse skin**

136 Next, we sought to examine whether commensal skin microbiota colonization could induce the
137 expression of *Sprr* family genes *in vivo*. *Sprr1b* is not expressed in mouse skin, so we tested
138 the ability of the microbiota to stimulate the expression of the mouse orthologs, *Sprr1a* and
139 *Sprr2*a. In contrast to what we observed in human sebocytes in culture, *Sprr* gene expression
140 was similar between germ free and conventional mice (Fig 2A), indicating that bacterial
141 colonization alone is insufficient to trigger increased expression of *Sprr* genes in mouse skin.
142 As sebaceous glands cells are located deeper in the dermis, we next chose to test whether
143 intradermal injection of LPS – mimicking wounding and infection conditions — could
144 stimulate *Sprr1a* and *Sprr2a* expression in mouse skin. Indeed, qRT-PCR analysis revealed that
145 intradermal injection of LPS stimulates the expression of *Sprr1a* and *Sprr2a* in mouse skin (Fig
146 2B). Canonically, LPS stimulates gene expression through activation of TLR4 and the TLR
147 signaling adaptor MYD88. Thus, LPS injected into the skin of *Myd88*$^{-/-}$ mice did not trigger
148 increased expression of the *SPRR* genes (Fig 2B), indicating that LPS induces SPRR protein
149 expression through the TLR-MYD88 signaling pathway. Consistent with these data, both live
150 and heat-inactivated *Escherichia coli* (*E. coli*) bacteria were able to induce SPRR expression,
151 suggesting that stimulation of *Sprr1a* and *Sprr2a* in mouse skin does not depend on the presence
152 of bacterial metabolites (Fig 2C). As has been shown by others [21], we also found that *Sprr1a*
153 and *Sprr2a* transcript abundance is locally induced by crosshatch skin wounding in mice (Fig
154 2D).

155 Next, to investigate the expression pattern of SPRR proteins in mouse skin, we performed
156 immunofluorescence experiment using a commercial antibody specific to SPRR1A. SPRR1A
157 is expressed in the sebaceous gland and non-specifically at the junction of the sebaceous gland
158 and hair follicle (Fig 2E). This suggests SPRR proteins expressed in the sebocyte may be
159 secreted to the hair canal and are present at the skin surface. Since our immunofluorescence
160 images and prior studies in keratinocytes indicated that SPRR1A and SPRR2A are expressed
161 by keratinocytes [22,23], we sought to study whether LPS could stimulate SPRRs expression in
162 keratinocyte cells. We first made use of hTert cells originally derived from human foreskin
163 keratinocytes and immortalized by expression of human telomerase and mouse Cdk4 and
164 treated the hTert cells with LPS for 24 hours. The qRT-PCR results showed that LPS cannot
165 induce the expression of *SPRR* family genes in human keratinocytes (fig S4). To further
166 confirm this result, we isolated primary mouse keratinocytes from neonatal mice, and cultured
167 them under both low and high calcium condition. Under low calcium conditions the
168 keratinocyte cell can proliferate but won't differentiate into a stratified layer. High calcium did
169 initiate the differentiation process and triggered increased expression of both mouse *Sprr1a* and
170 *Sprr2a* (fig S5). However, LPS did not stimulate the expression of *Sprr* genes in mouse
171 keratinocyte under either condition (fig S5). Taken together, these data show that SPRR
172 proteins are unregulated by LPS in human sebocytes in culture and by LPS dermal injection in
173 mouse skin.

174 **SPRR proteins are bactericidal against skin pathogens and commensals**

175 The SPRR family proteins have highly conserved amino acid sequences with numerous
176 cysteine and proline repeats. The antimicrobial properties of proline rich proteins have not been
177 described in humans. However, in insects and lower vertebrates, proteins rich in cysteines and
178 prolines have been shown to kill microbes [24,25]. Based on these findings, we hypothesized that
179 the SPRR proteins might function in cutaneous host defense as antimicrobial proteins. To test
180 the antimicrobial ability of SPRR proteins, we produced recombinant human SPRR1B,
181 SPRR2A and mouse SPRR1A protein in the baculovirus insect cell expression system and
182 further purified to homogeneity using size exclusion chromatography (fig S6). We then tested
183 the antimicrobial function of SPRR proteins against skin commensals and pathogens *in vitro.*
184 When bacteria were exposed to SPRR proteins, we observed a marked dose-dependent
185 reduction in the viability of *Staphylococcus epidermidis* (*S. epidermidis*), Methicillin Resistant
186 *Staphylococcus aureus* (MRSA), and *P. aeruginosa* (Fig 3A). with is a more than 90% decline
187 in bacterial viability after 2-hour exposure to 2.5 μM of SPRR proteins (Fig 3B). In contrast,
188 SPRR proteins had no impact on the viability of the prototypical Gram-negative bacteria
189 *Escherichia coli* (fig S7). Lastly, to visualize morphological changes of *P. aeruginosa* after
190 exposure to SPRR proteins, we used transmission electron microscopy and observed distinct
191 bacterial cell membrane damage and cytoplasmic leakage (Fig 3C).
192 Since SPRR proteins exhibit similar spectrum of bactericidal activity, we chose to use human
193 SPRR1B and mouse SPRR1A protein to further delineate the mechanism underlying its
194 bactericidal activity. We first used the propidium iodide (PI) uptake assay to assess the capacity
195 of SPRR proteins to permeabilize bacterial membranes. Human SPRR1B and mouse SPRR1A

196 proteins promoted the dose-dependent uptake of the membrane-impermeant small molecule
197 dye, PI, by *P. aeruginosa* (Fig 3D). Next, we examined whether SPRR proteins can directly
198 bind lipid molecules by incubating proteins with lipid strips dotted with different lipids. Both
199 human SPRR1B and mouse SPRR1A bind to lipids bearing negatively charged lipid head
200 groups, but not to neutral lipids (Fig 3E). These data are consistent with the idea that most
201 bacterial cell membranes are negatively charged and thus susceptible to SPRR1 binding. Lastly,
202 to determine whether SPRR proteins disrupt bacterial membrane, we incubated human
203 SPRR1B and mouse SPRR1A protein with liposomes loaded with the fluorescent dye
204 carboxyfluorescein (CF, ~10 Å Stokes diameter) and quantified dye release after exposure.
205 Phosphatidylcholine (PC)/ phosphatidylserine (PS) liposomes are composed of 85% of the
206 neutral lipid PC and 15% of the negatively charged lipid PS —similar to that of bacterial
207 membranes. Both human SPRR1B and mouse SPRR1A protein induced rapid dye efflux from
208 negatively charged PC/PS liposomes in a dose-dependent manner (Fig. 3F). These findings
209 confirm that SPRR proteins exert bactericidal activity through membrane disruption. Taken
210 together, these results suggest that SPRR proteins are bactericidal and compromise the
211 membrane of specific skin bacteria including the pathogen *P. aeruginosa*.

212 **SPRR proteins limit MRSA and *P. aeruginosa* infection**

213 Given that SPRR1A and SPRR2A protein exhibited bactericidal activity against a panel of skin
214 pathogens *in vitro* (Figure 3), we predicted that the removal of these proteins might limit MRSA
215 and *P. aeruginosa* skin infection *in vivo*. To test this hypothesis, we created mice lacking
216 SPRR1A and SPRR2A. We used a CRISPR/Cas9-mediated in vitro fertilization method to

217 delete the entire mouse *Sprr1a* locus of the *Sprr2a*$^{-/-}$ mice [26] and verified that SPRR1A and
218 SPRR2A are absent in *Sprr1a*$^{-/-}$;*Sprr2a*$^{-/-}$mice skin at both the transcript and protein level (fig
219 S8). *Sprr1a*$^{-/-}$;*Sprr2a*$^{-/-}$ mice were healthy and showed normal skin barrier with no signs of
220 immune infiltration and no significant change in transepidermal water loss (TEWL) (fig S9).
221 To test the *Sprr1a*$^{-/-}$;*Sprr2a*$^{-/-}$ mice for susceptibility to infection, we inoculated the skin of
222 wild-type and *Sprr1a*$^{-/-}$;*Sprr2a*$^{-/-}$ mice with 1 x 10^6 CFU of a bioluminescent strain of MRSA
223 by topical application. The luminescence was monitored daily with serial photography and
224 quantified for 3 consecutive days (Fig 4A). Mice devoid of SPRR1A and SPRR2A expression
225 had greater bacterial burdens in the first 3 days of MRSA infection (Fig 4B, 4C). Next, we
226 aimed to assess the susceptibility of *Sprr1a*$^{-/-}$;*Sprr2a*$^{-/-}$ mice to *P. aeruginosa* skin infection.
227 Since damaged or burned skin has increased risk of *P. aeruginosa* infection [7], we first
228 introduced skin wounding in mice by superficial crosshatching method, and then inoculated 1
229 x 10^6 CFU of a bioluminescent strain of *P. aeruginosa* at the wounding site. Intravital imaging
230 and quantification revealed that *Sprr1a*$^{-/-}$;*Sprr2a*$^{-/-}$ mice are more susceptible to *P. aeruginosa*
231 skin infection (Fig 4D-4F). Collectively, we confirm that SPRR proteins limit MRSA and *P.*
232 *aeruginosa* infection in mice skin.
233
234 **Discussion**
235
236 Skin is in direct contact with the microbe-filled outer world. Thus, defending the host from
237 invasion by pathogens like *S. aureus* and *P. aeruginosa* is one of the chief functions of the skin
238 [6,27]. In this study we have identified SPRR1 and SPRR2 proteins as a previously uncharacterized

239 group of antibacterial proteins expressed by keratinocytes and sebaceous gland cells, which can
240 rapidly kill pathogens through membrane disruption and limit bacterial skin infection.
241 Several earlier studies have shown that SPRR proteins are upregulated in the GI tract, urinary
242 tract and the airway after exposure to stress and other inflammatory stimuli [28]. Further, Hu et
243 al. recently revealed that SPRR2A has antimicrobial actions in the gastrointestinal tract during
244 helminth infection [26]. Our data highlight a previously unappreciated role of SPRR family
245 proteins in skin immune defense, demonstrating that both SPRR1 and SPRR2 are bactericidal
246 proteins induced in sebocytes by the bacterial cell wall component LPS (Fig 1). The major role
247 of sebaceous glands in mammals is to produce sebum, a mixture of non-polar lipids and proteins
248 required for normal skin ecology [29]. Sebum secretion can also act as a delivery system for AMPs
249 [30]. Though beneficial to the host, AMPs can damage mammalian membranes, so confining
250 expression of AMPs to the non-viable parts of skin through sebum delivery is optimal. Sebum
251 also excretes AMPs to the surface within an acidic milieu, which is often required for AMP
252 activity [31].
253 Interestingly, our data also show that bacterial colonization of germ-free mice did not
254 induce expression of SPRR proteins *in vivo* (Fig 2). Further, LPS was not able to stimulate the
255 production of SPRR proteins in mouse keratinocytes (fig S4-5). Taken together, our findings
256 suggest that deeper penetration of bacterial stimuli may be required for MYD88 mediated
257 SPRR protein production in skin. These finding are distinct from what has been observed in the
258 gastrointestinal tract, where colonization of germ-free mice is sufficient to stimulate SPRR2A
259 expression [32]. As SPRR family proteins also function as cross-linking proteins in terminal

260 differentiation of keratinocytes and formation of the cornified cell envelope (Candi et al., 2005),
261 there are likely other regulatory networks that control SPRR proteins expression in skin in
262 response to wounding and other stimuli. Additional studies with sebaceous gland-specific
263 deletion of TLRs and MYD88 will be required to confirm that stimulation of SPRR proteins by
264 LPS requires interaction with TLRs on sebocytes.

265 In this study, we also reveal that SPRR family proteins have potent bactericidal activity
266 against *Staphylococcal* species and the gram-negative bacteria *P. aeruginosa* (Fig 3A-C), with
267 effective inhibition at low micromolar concentrations. Further, our biochemical data show that
268 mouse and human SPRR1 proteins interact with negatively charged lipid membranes,
269 suggesting broad spectrum antimicrobial capability of these proteins (Fig 3D-F). Additionally,
270 skin devoid of SPRR1 and SPRR2 is more susceptible to skin infection by MRSA and
271 *Pseudomonas aeruginosa,* both pathogens that cause skin infections requiring hospitalization
272 (Fig 4). Treatments for these infections are currently limited. SPRR proteins might be
273 promising alternatives to traditional antibiotics used to cure MRSA or *P. aeruginosa* infection.

274 Human SPRR proteins are 6–18 kDa in size and comprise four subclasses (SPRR1,
275 SPRR2, SPRR3, and SPRR4) with a similar structural organization. Among them, two SPRR1
276 and seven SPRR2 proteins are characterized with a much higher homogeneity, as they contain
277 a similar consensus repeat sequence [18]. Our findings that SPRR family proteins have
278 antimicrobial function may have implications for other proline-rich proteins expressed at other
279 mucosal sites. Altogether, these findings expand our current understanding of the molecules

280 involved in cutaneous host defense and provide insight into how the sebaceous gland
281 contributes to the fight against skin infection.
282
283
284 **Materials and Methods**
285 **Mice**
286 All animal protocols were approved by the Institutional Animal Care and Use Committees of
287 the University of Texas (UT) Southwestern Medical Center. Age- and sex-matched mice 8-12
288 weeks old were used for all experiments. Conventionally raised C57BL/6 wild type (WT),
289 Myd88$^{-/-}$ and *Sprr1a*$^{-/-}$;*Sprr2a*$^{-/-}$ on C57BL/6 background were bred and maintained in the
290 specific pathogen free (SPF) barrier facility at the UT Southwestern Medical Center on standard
291 chow diet. The generation of *Sprr1a*$^{-/-}$;*Sprr2a*$^{-/-}$ mice is described below. Germ-free (GF)
292 C57BL/6 mice were bred and maintained in flexible film vinyl isolators in the gnotobiotic
293 mouse facility at UT Southwestern with autoclaved diet (Hooper Lab Diet 6F5KAI, Lab Diet,
294 St. Louis, MO) and autoclaved nanopore water. All mice were housed under a 12 hour light-
295 dark cycle, and mice were randomly assigned to treatment groups.
296
297 *Sprr1a*$^{-/-}$;*Sprr2a*$^{-/-}$ mice were generated using CRISPR/Cas9-mediated *in vitro* fertilization
298 with a guide RNA targeting regions upstream and downstream of the *Sprr1a* locus on the
299 basis of *Sprr2a*$^{-/-}$ mice (Figure S8). *Sprr2a*$^{-/-}$ mice were obtained with the permission of Dr.
300 Lora Hooper [26]. Guide RNAs were injected into fertilized female *Sprr2a*$^{-/-}$ mice embryos
301 by the UT Southwestern Transgenic Core facility. The resulting litters were screened by

302 genomic sequencing to detect the deletion of *Sprr1a* and *Sprr2a* locus. Mice harboring the
303 deleted allele were backcrossed with WT to homozygosity.
304
305 **Bacterial strains**
306 Bacteria were grown in species-specific growth media: *Escherichia coli* (ATCC; ATC-PTA-
307 7555) and *Citrobacter rodentium* (ATCC51459) were grown in Luria Broth. *Pseudomonas*
308 *aeruginosa* (ATCC27853), bioluminescent *Pseudomonas aeruginosa* strain Xen05 (Perkin
309 Elmer 119228) and *Enterococcus faecalis* (ATCC29212) were grown in Brain Heart Infusion
310 Broth (BD Biosciences). Methicillin resistant *Staphylococcus aureus* (ATCC25923),
311 bioluminescent MRSA strain SAP430 *lux* [33], *Staphylococcus epidermidis* (clinical isolate),
312 *Staphylococcus xylosus* (clinical isolate) were grown in Tryptic Soy Broth.
313
314 **Sebocyte cell culture and treatments**
315 SZ95 cells are an immortalized human sebocyte cell line generated from the face of an 87-year-
316 old female and transformed with Simian virus 40. These cells were previously obtained from
317 Cristos Zouboulis [14]. SZ95 sebocytes were maintained in Sebomed Basal Medium (Fischer
318 Scientific NC9711618) supplemented with 10% fetal bovine serum (GeminiBio 100-106), 5
319 ng/ml human epidermal growth factor (ThermoFisher PHG0313) and 1% Antibiotic-
320 Antimycotic (Gibco 15240062). Cells were cultured in 5% CO_2 incubator at 37°C. Cells were
321 stimulated with 1μg/ml LPS (Sigma L4524). 16 hours post-stimulation cells were harvested
322 and analyzed as described below. For TLR agonists treatment, reagents in human TLR1-9

323 Agonist kit (InvivoGen, tlrl-kit1hw) were diluted to working concentration in PBS. 100ng/ml
324 Pam3CSK4, 1 x 10^8 cells/ml HKLM, 500ng/ml Poly (I:C), 500ng/ml Flagellin, 100ng/ml FSL-
325 1 and 1μg/ml Imiquimod were used for stimulation of SZ95 cells. For heat-inactivated bacteria
326 treatment, bacteria were grown to mid-logarithmic phase, spun down, washed and resuspended
327 in PBS. Bacteria were heat-inactivated by incubation at 95 ^{o}C for 20 minutes. Then 1 x10^8
328 cells/ml were used for each treatment.
329
330 **Immunofluorescence microscopy**
331 Mouse skin samples were fixed in formalin and embedded in paraffin by the UT Southwestern
332 histology core. Samples were deparaffined with xylene followed by rehydration with
333 decreasing concentrations of ethanol. Boiling in 10mM sodium citrate buffer with 0.2% tween
334 for 15 minutes for antigen retrieval. Slides were blocked with 10% FBS, 1% BSA and 1%
335 Triton X-100 in PBS, and then incubated with primary antibodies against mouse SPRR1A
336 (Thermo Fisher PA5-26062), mouse CD36 (R&D AF2519), rabbit IgG isotype control (Thermo
337 Fisher 02-6102) or goat IgG isotype control (Thermo Fisher 02-6202) using 1:100 dilutions at
338 4°C overnight. Secondary antibodies Alex Fluor 594 or Alexa Fluor 647 (Thermo Fisher) were
339 diluted 1:350 in blocking buffer and applied to slides for 1 hour at room temperature in the
340 dark. Slides were then washed with PBST (PBS with 0.2% tween) and mounted with DAPI
341 Fluoromount-G (Southern Biotechnology 0100-20). Images were captured using an Echo
342 Revolve 4 microscope.
343

344 **Quantitative real-time PCR**

345 RNA was extracted from cells or mouse skin using the RNAeasy Plus universal kit (Qiagen
346 73404). RNA was quantified by absorbance at 260 nm, and its purity was evaluated by the
347 ratios of absorbance at 260/280 nm. 2µg of RNA was used for cDNA synthesis (Thermofischer
348 4368814, High Capacity cDNA reverse transcription kit). Quantitative real-time PCR was
349 performed using PowerUp SYBR Green Gene Expression Assays (Thermofischer A25741) and
350 a QuantStudio 7 Flex Real-Time PCR System (Applied Biosystems). Relative expression
351 values were calculated using the comparative Ct (ΔΔCt) method, and transcript abundances
352 were normalized to GAPDH transcript abundance. The primer sequences are shown in table
353 S1.

354

355 **Whole transcriptome sequencing and data analysis**

356 RNA was extracted from SZ95 sebocyte cells using the RNAeasy Plus universal kit (Qiagen
357 73404). RNA quality was assessed using Agilent 2100 Bioanalyzer. Truseq RNA sample
358 preparation kit v2 (Illumina) was used for the preparation of sequencing libraries. Sequencing
359 was performed on an Illumina HiSeq 2500 for signal end 50 bp length reads. Sequence reads
360 were mapped against the hg19 genome using TopHat. For each gene, read counts were
361 computed using HTSeq-count and analyzed for differential expression using DESeq2.

362

363 **Western blot**

364 SZ95 cells were harvested by applying 200 µL of diluted 1x sample buffer (Thermo Fisher
365 39000) directly to a 6-well plate, scraping down the cell sample to disrupt the membranes, then
366 boiling for 15 minutes before loading. Equal amounts of protein were loaded onto a 4-20%
367 gradient SDS-PAGE and transferred to a PVDF membrane. After blocking with 5% milk in
368 TBST, the membranes were incubated with anti-SPRR1B antibody (Thermo Fisher PA5-
369 26062), anti-SPRR2A (Abcam ab125385) or anti-GAPDH (Abcam ab181602) at 4ºC
370 overnight. Membranes were then incubated with anti-rabbit secondary antibodies conjugated
371 with HRP (Abcam). Membranes were visualized using a Bio-Rad ChemiDoc Touch system
372 and bands were quantified by Image Lab software.
373
374 **Keratinocyte cell line culture and treatments**
375 hTERT (ATCC CRL-4048) and primary mouse keratinocyte cells were cultured in KSFM
376 medium (Invitrogen, 37010022) supplemented with 0.05 mM $CaCl_2$ (Sigma, C7902), 0.05
377 µg/mL hydrocortisone (Sigma, H0888), 5 ng/mL EGF (Invitrogen, 10450-013), 7.5 µg/mL
378 bovine pituitary extract (Invitrogen, 13028-014), 0.5 µg/mL insulin (Sigma, I9278), 100 U/mL
379 penicillin, 100 µg/mL streptomycin, and 25 µg/mL of amphotericin B (Invitrogen, 10450-013).
380 Mouse primary keratinocytes were isolated through dispase digestion. Before digestion, the
381 subcutaneous fat was first removed from the mouse skin. Skin tissue from 3-5 days neonatal
382 mice was floated on 1 U/ml dispase (Corning, 354235) in HBSS (Gibco, 14170) for 16 h at 4°C
383 with the dermis side down. The next day, the skin was placed in a new dish with the epidermis
384 side down, and the epidermis was peeled and placed into a new dish with HBSS. After being

385 washed, the cells were collected into a new 15 mL tube. The epidermis was cut into small
386 pieces, resuspended in HBSS, gently pipetted up and down several times, and then combined
387 with the cells in the 15 mL tube. The cell solution was filtered with a 70 μm cell strainer,
388 centrifuged at 1,000 rpm for 4 minutes, and resuspended in complete KSFM medium. The cells
389 were gently washed once and seeded in culture dishes with complete KSFM medium. The
390 culture dishes were precoated with collagen (Advanced Biomatrix, 5005-B). Keratinocytes
391 from each mouse were seeded in one 10 cm dish, and fresh complete KSFM medium was
392 supplied after 24 hours. After 3-4 days, the primary keratinocytes reached approximately 80%
393 confluence under normal culture conditions in a 5% CO_2, 37°C incubator. For keratinocyte
394 differentiation, cells were treated with 1 mM $CaCl_2$ for 2 days. For treatment of keratinocyte
395 cells, 1 μg/mL LPS (Sigma L4524) were supplemented in the KSFM complete medium. 16
396 hours post-stimulation cells were harvested for qRT-PCR or Western blot analysis.
397
398 **Intradermal injection of mice**
399 The mouse dorsal hair was removed by shaving (Andis ProClip), followed by depilatory cream
400 (Nair™) one day before injection. LPS (Sigma L4524) was dissolved in PBS and further diluted
401 to a concentration of 1 mg/mL. For intradermal injection of LPS, each mouse was injected with
402 50 μL of LPS solution to the back skin. For intradermal injection of bacteria, various bacteria
403 were grown in species-specific media to mid-logarithmic phase, spun down, washed and
404 resuspended in PBS to a concentration of 1 $x10^8$ cells/mL. Bacteria were heat-inactivated by
405 incubation at 95 °C for 20 minutes. 100 μL of live or heat-inactivated bacteria was injected to

406 the mouse back skin. The site of injection was circled with permanent marker. After 8 hours,
407 mice were sacrificed and the injection site skin was analyzed.
408
409 **Protein expression and purification**
410 *SPRR* genes containing a C-terminal 6xHis tag were cloned into a pFastBac1 vector and
411 heterologously expressed in Sf9 cells (Thermo Fisher). One liter of cells (2.5×10^6 cells/mL)
412 was infected with 10 mL baculovirus at 28°C. Cells were cultured in suspension and harvested
413 48 hours after infection. Harvested cells were resuspended in the buffer containing 25 mM Tris-
414 HCl pH 8.0, 150 mM NaCl and 1 mM Phenylmethylsulfonyl fluoride (PMSF), and lysed by
415 sonication. The mixture was pelleted by centrifugation at 10,000*g* for 30 minute and the
416 supernatant was loaded onto a Ni^{2+} metal affinity column (Qiagen). The column was washed
417 with buffer containing 30 mM imidazole and the protein was eluted in buffer containing 300
418 mM imidazole. The eluate was concentrated in a 3K cutoff Amicon Ultra centrifugal device
419 (Millipore) and further purified by size exclusion chromatography on a Superdex 75™ 10/300
420 GL column (GE Healthcare Life Sciences) in standard assay buffer (10 mM MES, pH 6.0 and
421 25 mM NaCl).
422
423 **Bacterial killing assays**
424 Bacteria were grown in species-specific growth media as described above. 10 mL bacterial
425 cultures were grown to mid-logarithmic phase and then pelleted and washed twice in assay
426 buffer (10 mM MES, pH 6.0, 25 mM NaCl). Approximately 5 $\times10^6$ cells/mL bacteria were then

427 incubated at 37°C for 2 hours in assay buffer with varying concentrations of recombinant SPRR
428 protein or BSA (Gemini 700-106P). Surviving colony-forming units (CFU) were quantified by
429 dilution plating onto agar plates and calculated as a percentage of the remaining colonies in the
430 assay buffer only control sample.
431
432 **Lipid strip assay**
433 Membrane lipid strips (Echelon, P-6002) were used following the manufacturer's protocol.
434 Briefly, the lipid strips were blocked with blocking buffer (10 mM MES, pH 6.0, 25 mM NaCl,
435 2% BSA, and 0.05% Tween-20) for 1 hour at room temperature. Purified recombinant SPRR
436 proteins were diluted to 1 μg/mL in blocking buffer and incubated with the lipid strip overnight
437 at 4°C. After three washes with washing buffer (10 mM MES, pH 6.0, 25 mM NaCl and 0.05%
438 Tween-20), the lipid strip was sequentially incubated with anti-SPRR1B antibody and HRP-
439 conjugated secondary antibody. Dots were detected with ECL reagent (Bio-Rad, 1705060)
440 using a Bio-Rad ChemiDoc system.
441
442 **Electron microscopy**
443 For electron microscopy of bacteria, 10 mL *P. aeruginosa* cultures were grown to mid-
444 logarithmic phase and then pelleted and washed in 10 mL standard assay buffer (10 mM MES
445 pH 6.0 and 25 mM NaCl). Bacteria were then resuspended in 1 mL standard assay buffer.
446 Purified recombinant SPRR proteins was added at a final concentration of 5 μM to 300 μL of
447 resuspended bacteria and incubated at 37°C for 2 hours. Bacteria were centrifuged for 10

448 minutes at 16,000 g, resuspended in cross-linking reagent (4% paraformaldehyde and 4%
449 glutaraldehyde in 0.1 M sodium phosphate buffer, pH 7.4), and incubated overnight at 4°C.
450 After three washes, bacterial pellets were embedded in 3% agarose, sliced into small blocks (1
451 mm^3), and fixed with 1% osmium tetroxide and 0.8% potassium ferricyanide in 0.1 M sodium
452 phosphate buffer for 1.5 hours at room temperature. Cells were rinsed with water then stained
453 with 1% uranyl acetate in water for 1 hour. Cells were dehydrated with increasing
454 concentrations of ethanol, transitioned into propylene oxide, infiltrated with Embed-812 resin,
455 and polymerized overnight in a 60°C oven. Blocks were sectioned with a diamond knife
456 (Diatome) on Leica Ultracut 7 ultramicrotome (Leica Microsystems), collected onto copper
457 grids, and post-stained with 2% aqueous uranyl acetate and lead citrate. Images were captured
458 on a Tecnai G2 spirit transmission electron microscope (Thermo Fisher) equipped with a LaB6
459 source using a voltage of 120 kV.
460
461 **Liposome disruption assay**
462 Unilamellar liposomes were prepared using lipids from Avanti. 85% 1-palmitoyl-2-oleoyl-
463 *sn*-glycero-3-phosphocholine or POPC (AVANTI PC #850457C) and 15% 1,2-dioleoyl-
464 *sn*-glycero-3-phospho-L-serine or DOPS (AVANTI PS #840035C) dissolved in chloroform
465 were mixed in specific molar ratios in glass tubes and then dried under a stream of N_2, followed
466 by drying under vacuum overnight to ensure complete removal of organic solvents. Dried lipids
467 were then combined with 5(6)-carboxyfluorescein (CF) (Sigma #21877) and vortexed for 5
468 minutes. Lipids were transferred to 2 mL cryotubes and subjected to five freeze thaw cycles in

469 liquid N_2 and stored at −80 °C freezer. Lipids were then thawed and passed through a 100
470 nm pore membrane using a mini-extruder kit (Avanti Polar Lipids #610000) and purified
471 on a PD-10 column to remove excess dye. Prepared liposomes were diluted in standard
472 assay buffer (10 mM MES, pH 6.0, 25 mM NaCl) to a working concentration of 100 μM.
473 QuantaMaster 300 fluorometer (Photon Technology International) was used to monitor
474 fluorescence. SPRR protein was added to the system at increasing concentrations. At the
475 end time point, 1% v/v n-octylglucoside detergent (OG, Anatrace #O311) was added to
476 completely disrupt the liposomes. Fluorescence was measured over time in seconds and as
477 a percentage of total CF dye released by the detergent OG.
478
479 **Dye uptake assay**
480 Bacterial cultures were grown to mid-logarithmic phase and then pelleted and washed in
481 standard assay buffer (10 mM MES, pH 6.0 and 25 mM NaCl). Bacteria were then diluted to
482 approximately 5 x 10^8 cells/mL in standard assay buffer containing 5.5 μg/mL Propidium iodide
483 (PI) (Thermo Fisher, P3566). Then bacterial samples (90 μL each well) were added to black
484 96-well Costar plates (Fisher, 07-200-567) and placed into a Spectramax plate reader
485 (Molecular Devices) that was pre-equilibrated to 37°C for 10 minutes. After an initial reading,
486 10 μL of recombinant purified SPRR proteins at varying concentrations or BSA were added
487 and fluorescence outputs (excitation, 535 nm; emission, 617 nm) were measured every 5
488 minutes for 1 hour. PI uptake activity was measured against the maximum fluorescence output
489 from the positive control added with 0.05% SDS.

490

491 **Skin infections**

492 The dorsal hair was removed from C57BL6 *Sprr1a*$^{-/-}$;*Sprr2a*$^{-/-}$ or WT male mice by shaving
493 (Andis ProClip), followed by depilatory cream (Nair). For MRSA infection, one day after
494 shaving, bioluminescent MRSA strain SAP430-*lux* were grown to mid-logarithmic phase in
495 Tryptic Soy Broth and then pelleted and washed twice in PBS. Approximately 1 x 10^6 CFU
496 bacteria in 100 µL PBS were placed on rectangular gauze. For *P. aeruginosa*- infection, after
497 24 hours, the dorsal skin was superficially abraded in a crosshatch pattern by a 15-blade scalpel
498 (Fine Scientific Tools 10115-10) to introduce skin wounding. One day post-wounding, the
499 bioluminescent *P. aeruginosa* strain Xen05 (Perkin Elmer 119228) were grown in Brain Heart
500 Infusion Broth (BD Biosciences) and around 1 x 10^6 CFU bacteria in 100 µL PBS were placed
501 on a gauze rectangle. The gauze was applied to the dorsal skin of *Sprr1a*$^{-/-}$;*Sprr2a*$^{-/-}$ or WT
502 mice and held in place with 2 tegaderm (3M 9505W) and a Band-Aid Sheer Strips (BAND-
503 AID) for 3 days. The luminescent was monitored daily with serial photography and
504 quantification using a IVIS Lumina3 imager machine.

505

506 **TEWL measurement**

507 Transepidermal water loss (TEWL) of mice dorsal skin was measured using Vapometer (Delfin
508 Technologies) according to manufacturer instructions.

509

510 **Data availability**

511 RNA-seq data (Figures 1B,1C) has been submitted to the Gene Expression Omnibus with an
512 accession number: GSE182756
513
514 **Statistical analysis**
515 Statistical details of experiments can be found in the figure legends, including how significance
516 was defined and the statistical methods used. Data represent mean ± standard error of the mean.
517 Formal randomization techniques were not used; however, mice were allocated to experiments
518 randomly and samples were processed in an arbitrary order. Mouse skin samples that were
519 determined to be in the anagen hair cycle were excluded. All statistical analyses were performed
520 with GraphPad Prism software. To assess the statistical significance of the difference between
521 two treatments, we used two-tailed Student's t-tests. To assess the statistical significance of
522 differences between more than two treatments, we used one-way ANOVAs.
523
524 **Acknowledgements**:
525 We would like to thank Dr. Lora Hooper for helpful discussion and sharing *Sprr2a*$^{-/-}$ mice
526 strain. We thank Dr. Richard Wang for sharing the hTert immortalized human keratinocyte cell
527 line. We thank Dr. Zheng Kuang for his help with analysis of RNA-sequencing data. This work
528 was supported by a Harold Amos Award through the Robert Wood Johnson Foundation,
529 National Institutes of Health K08 award, a UT Southwestern Disease Oriented Clinical Scholars
530 Program award, and a Burroughs Wellcome Fund Career Award for Medical Scientists.
531

532 **Author Contributions**:

533 C.Z. designed and performed most experiments. Z.H. performed protein expression and
534 purification and liposome assays in fig S6 and Fig 5. A.L. performed skin infection experiments
535 in Fig 4. M.A. and M.E. provided technical assistance with the mouse experiments and assisted
536 with bacterial killing assays in Fig 3A, 3B. M.S. completed the dose response and time course
537 experiments in fig S1. C.C.Z revised the manuscript and is the original source of the SZ95 cells.
538 C.Z. and T.A.H. designed experiments, interpreted results, and wrote the manuscript.

539

540 **Declaration of Interests**

541 The authors declare no competing interests.

542 **Figure Legends**

543

544 **Fig. 1. The expression of *SPRR* family genes are up-regulated by lipopolysaccharide (LPS)**
545 **in human sebaceous gland cells.** (A) Schematic of facial skin derived immortalized human
546 SZ95 sebaceous gland cells treated with LPS for RNA sequencing. (B) Volcano plot with
547 significantly up-regulated genes (fold change>1.4 and adjusted *p* value<0.01) highlighted in
548 red (up regulated in LPS treated). (C) Heat map of significantly up-regulated genes, represented
549 as Z-scored RPKM (reads per kilo base per million reads). *SPRR1B, SPRR2A* and *SPRR2D* are
550 highlighted in red. (D) Reverse transcription-quantitative polymerase chain reaction (RT-
551 qPCR) analysis of *SPRR1B, SPRR2A* and *SPRR2D* transcript in the vehicle and LPS treated
552 human SZ95 sebocytes. (E) Western blot analysis of SPRR1B and SPRR2A was performed on
553 vehicle or LPS treated SZ95 cells. GAPDH was used as the loading control. (F) Quantification
554 of Western blot in (E). Means ± SEM are plotted, **P*<0.05, ***P*<0.01, ****P*<0.001 was
555 determined by unpaired t-test.

556

557 **Fig. 2. The expression of *SPRR* family genes are up regulated by LPS in mice.** (A-D) qRT-
558 PCR analysis of *Sprr1a* and *Sprr2a* gene expression in mouse dorsal skin tissue. (A) Germ-free
559 mice (GF) compared to conventionally raised mice (CV). (B) PBS treated mouse skin compared
560 to LPS intradermal injection mouse skin in WT or MYD88$^{-/-}$ mouse. (C) Mouse intradermally-
561 injected by vehicle (PBS), *E.coli* or heat-inactivated (HI) E.coli. (D) Untreated mouse skin
562 compared to wounded skin abraded in a crosshatch pattern by a 15-blade scalpel. Means ± SEM
563 are plotted. *P < 0.05; **P < 0.01; ****P < 0.0001ns, not significant by unpaired t test. (E)
564 Immunofluorescence staining of SPRR1A expression in mice skin. CD36 was used as marker
565 of sebocyte cells. Nuclei are stained with DAPI (Blue). Epidermis and sebaceous gland
566 indicated with an arrow. White dashed line separates the epidermis and dermis. Yellow dashed
567 line indicates the outline of SG. Scale bar, 50 μm.

568

569 **Fig. 3. SPRR family proteins exert bactericidal activity against various skin commensal**
570 **and pathogenic bacteria by membrane disruption.** (A) Increasing concentrations of purified
571 recombinant SPRR proteins were added to mid-logarithmic phase *MRSA*, *S. epidermidis*,
572 *P.aeruginosa* for 2 hours and surviving bacteria were quantified by dilution plating. (B) 2.5 μM
573 of SPRR proteins was added to midlogarithmic phase bacteria for 2 hours and surviving bacteria
574 were quantified by dilution plating. Remaining Colony forming units (CFUs) are expressed as
575 a percentage of untreated bacteria control. (C) Transmission electron microscopy of *P.*
576 *aeruginosa* after incubation with 5 μM purified recombinant SPRR proteins. BSA was used as
577 negative control. Examples of cell surface damage and cytoplasmic leakage are indicated with
578 red rectangular box. Upper scale bars, 500 nm. Lower scale bars, 100 nm. (D) Propidium iodide
579 (PI) uptake by *P. aeruginosa* in the presence of increasing concentrations of mouse SPRR1A
580 and human SPRR1B protein. (E) Membranes displaying various lipids were incubated with
581 1μg/mL SPRR proteins, and detected with specific antibody. (F) Carboxyfluorescein (CF)-
582 loaded liposomes were treated with increasing concentrations of mouse SPRR1A and human
583 SPRR1B protein, and dye efflux was monitored over time and was expressed as a percentage

584 of total efflux in the presence of the detergent octyl glucoside (OG). All assays were performed
585 in triplicate. Means ± SEM are plotted. *P < 0.05; ***P < 0.001; ****P < 0.0001; ns, not
586 significant by two-tailed t-test.
587
588
589 **Fig. 4. SPRR family proteins protect against skin MRSA and *P. aerugonisa* infection.** (A-
590 C) WT and *Sprr1a*$^{-/-}$;*Sprr2a*$^{-/-}$ mice were epicutaneously challenged with MRSA (1 x 10^6
591 CFU) on the shaved dorsal skin for 3 consecutive days. (A) Representative *in vivo*
592 bioluminescent imaging (BLI) photographs from Day 0 to Day 3. Quantification of MRSA total
593 flux (photons/s) for each mouse (B) or plotted as Means ± SEM (C). (D-F) WT and
594 *Sprr1a*$^{-/-}$;*Sprr2a*$^{-/-}$ mice were superficially abraded in a crosshatch pattern by a 15-blade
595 scalpel to introduce skin wounding. One day post crosshatch wounding, WT and
596 *Sprr1a*$^{-/-}$;*Sprr2a*$^{-/-}$mice were topically applied with 1 x 10^6 CFU *P. aerugonisa* on the back
597 skin for 3 days. (D) Representative in vivo bioluminescent imaging (BLI) signals from Day 0
598 to Day 3. Quantification of *P. aerugonisa* total flux (photons/s) for each mouse (E) or plotted
599 as Means ± SEM (F). *p < 0.05, ns, not significant by unpaired t-test.
600
601
602
603 **fig. S1. Dose response and time course analysis of LPS treatment on human sebocyte cells.**
604 qRT-PCR analysis of *SPRR1B and SPRR2A* transcript in the vehicle and various LPS treated
605 human SZ95 sebocytes. (A) SZ95 sebocyte cells were treated with different concentration of
606 LPS for 16 hours. (B) SZ95 cell were treated with 1 μg/mL LPS for different length of time.
607 Means ± SEM are plotted. **P < 0.01; ***P < 0.001;ns, not significant by unpaired t-test.
608
609 **fig. S2. The expression of SPRR family genes are up regulated by TLR2 and TLR4**
610 **agonists in human sebaceous gland cells.** (A) A list of different TLR agonists. (B) qRT-PCR
611 analysis of *SPRR* family genes expression in the vehicle and various TLR agonists treated SZ95
612 cells. Means ± SEM are plotted. *P < 0.05; **P < 0.01; ***P < 0.001; ****P < 0.0001; ns, not
613 significant by one-way ANOVAs.
614
615 **fig. S3. Gram-negative bacteria can trigger *Sprr2a* gene expression in human sebaceous**
616 **gland cells.** qRT-PCR analysis of *Sprr2a* transcript in the vehicle and various heat inactivated
617 bacteria treated human SZ95 sebocyte cells. Means ± SEM are plotted. ****P < 0.0001; ns, not
618 significant by one-way ANOVAs.

619
620 **fig. S4. LPS cannot induce the expression of *SPRR* family genes in human keratinocyte**
621 **cells.** hTERT immortalized human keratinocyte cells were treated with LPS for 16 hours. qRT-
622 PCR analysis of *SPRR1B, SPRR2A* and *SPRR2D* transcript in the vehicle and LPS treated
623 human hTERT keratinocytes. Means ± SEM are plotted. ns, not significant by unpaired t-test.
624
625 **fig. S5. LPS cannot trigger the expression of *Sprr* family genes in primary mouse**
626 **keratinocytes.** Primary mouse keratinocytes were isolated from 3-5 days old neonatal mice
627 through dispase digestion. With 0.05 mM $CaCl_2$ (Low Ca^{2+}), keratinocytes can proliferate but
628 won't differentiate into a stratified layer. Under 1 mM $CaCl_2$ (High Ca^{2+}) condition,
629 keratinocytes will initiate differentiation process. (A) qRT-PCR analysis of *Sprr1a* and *Sprr2a*
630 transcript in the vehicle and LPS treated primary mouse keratinocyte cells cultured under Low
631 Ca^{2+} or High Ca^{2+} condition. (B) Western blot analysis of SPRR1A protein was performed on
632 vehicle or LPS treated primary mouse keratinocytes under both Low Ca^{2+} and High Ca^{2+}
633 condition. (C) Quantification of the Western blot in (B). Means ± SEM are plotted. *P < 0.05;
634 ***P < 0.001 by unpaired t-test.
635
636 **fig. S6. Recombinant expression and purification of SPRR proteins.** (A and C)
637 Recombinant mouse SPRR1A protein (A) and human SPRR1B protein (C) was expressed using
638 a baculovirus expression system and purified by size-exclusion chromatography (Superdex 75
639 10/300 GL) [26]. (B and D) Fractions from (A) and (C) were visualized by Coomassie blue
640 staining following SDS-polyacrylamide gel electrophoresis (SDS-PAGE).
641
642 **fig. S7. SPRR1A protein was resistant to Gram-negative bacteria *Escherichia coli*.**
643 Increasing concentrations of purified recombinant mouse SPRR1A protein was added to mid-
644 logarithmic phase *Escherichia coli* for 2 hours and surviving bacteria were quantified by
645 dilution plating. Remaining Colony forming units (CFUs) are expressed as a percentage of
646 untreated bacteria control. BSA was used as negative control. Means ± SEM are plotted.
647
648 **fig. S8. Generation and validation of *Sprr1a*$^{-/-}$*;Sprr2a*$^{-/-}$ mice by CRISPR/Cas9 genomic**
649 **targeting.** (A) Schematic diagram of two-step strategy using CRISPR/Cas9-mediated gene
650 targeting to delete the entire *Sprr2a* and *Sprr1a* locus. (B) qRT-PCR analysis of *Sprr1a* and
651 *Sprr2a* expression in the skin of WT and *Sprr1a*$^{-/-}$*;Sprr2a*$^{-/-}$ mice. Values were normalized to
652 *Gapdh* expression. Means ± SEM are plotted. *P < 0.05; ***P < 0.001 by unpaired t-test. (C)
653 Western blot analysis of SPRR1A protein in the skin of WT and *Sprr1a*$^{-/-}$*;Sprr2a*$^{-/-}$mice.
654 GAPDH was used as the loading control.
655
656 **fig. S9. *Sprr1a*$^{-/-}$*;Sprr2a*$^{-/-}$ mice does not show signs of inflammation or impaired skin**
657 **barrier.** (A) Transepidermal water loss (TEWL) of WT and *Sprr1a*$^{-/-}$*;Sprr2a*$^{-/-}$mice skin was
658 analyzed. Means ± SEM is plotted, ns, not significant by unpaired t test. (B) Representative
659 H&E staining of mouse skin from WT and *Sprr1a*$^{-/-}$*;Sprr2a*$^{-/-}$. Scale bar, 200 μm.
660

References:

1. Belkaid, Y. & Segre, J. A. Dialogue between skin microbiota and immunity. *Science* (2014) doi:10.1126/science.1260144.

2. Duerkop, B. A. & Hooper, L. V. Resident viruses and their interactions with the immune system. *Nature Immunology* (2013) doi:10.1038/ni.2614.

3. Oh, J., Byrd, A. L., Park, M., Kong, H. H. & Segre, J. A. Temporal Stability of the Human Skin Microbiome. *Cell* **165**, 854–866 (2016).

4. Findley, K. *et al.* Topographic diversity of fungal and bacterial communities in human skin. *Nature* (2013) doi:10.1038/nature12171.

5. Dryden, M. S. Skin and soft tissue infection: microbiology and epidemiology. *Int. J. Antimicrob. Agents* (2009) doi:10.1016/S0924-8579(09)70541-2.

6. Stulberg, D. L., Penrod, M. A. & Blatny, R. A. Common bacterial skin infections. *Am. Fam. Physician* (2002) doi:10.1080/00325481.1993.11701692.

7. Huebinger, R. M. *et al.* Targeting bacterial adherence inhibits multidrug-resistant Pseudomonas aeruginosa infection following burn injury. *Sci. Rep.* **6**, 1–8 (2016).

8. Klevens, R. M. *et al.* Invasive methicillin-resistant Staphylococcus aureus infections in the United States. *J. Am. Med. Assoc.* (2007) doi:10.1001/jama.298.15.1763.

9. Zhang, L. J. & Gallo, R. L. Antimicrobial peptides. *Current Biology* (2016) doi:10.1016/j.cub.2015.11.017.

10. Nakatsuji, T. & Gallo, R. L. Antimicrobial peptides: Old molecules with new ideas. *Journal of Investigative Dermatology* (2012) doi:10.1038/jid.2011.387.

11. Mukherjee, S. *et al.* Antibacterial membrane attack by a pore-forming intestinal C-type lectin. *Nature* (2014) doi:10.1038/nature12729.

12. Mishra, A. K., Choi, J., Moon, E. & Baek, K. H. Tryptophan-rich and proline-rich antimicrobial peptides. *Molecules* (2018) doi:10.3390/molecules23040815.

13. Gallo, R. L. & Hooper, L. V. Epithelial antimicrobial defence of the skin and intestine. *Nature Reviews Immunology* vol. 12 503–516 (2012).

14. Harris, T. A. *et al.* Resistin-like Molecule a Provides Vitamin-A- Dependent Antimicrobial Protection in the Skin Article Resistin-like Molecule a Provides Vitamin-A-Dependent Antimicrobial. *Cell Host Microbe* **25**, 1–12 (2019).

15. Fischer, H. *et al.* Holocrine Secretion of Sebum Is a Unique DNase2-Dependent Mode of Programmed Cell Death. *J. Invest. Dermatol.* **137**, 587–594 (2017).

16. Zouboulis, C. C., Yoshida, G. J., Wu, Y., Xia, L. & Schneider, M. R. Sebaceous gland: Milestones of 30-year modelling research dedicated to the "brain of the skin". *Exp. Dermatol.* (2020) doi:10.1111/exd.14184.

17. Zouboulis, C. C. *et al.* Beyond acne: Current aspects of sebaceous gland biology and function. *Reviews in Endocrine and Metabolic Disorders* (2016) doi:10.1007/s11154-016-9389-5.

18. Cabral, A. *et al.* Structural Organization and Regulation of the Small Proline-rich Family of Cornified Envelope Precursors Suggest a Role in Adaptive Barrier Function. *J. Biol. Chem.* (2001) doi:10.1074/jbc.M100336200.

19. Candi, E., Schmidt, R. & Melino, G. The cornified envelope: A model of cell death in the skin. *Nature Reviews Molecular Cell Biology* vol. 6 328–340 (2005).

20. Vaishnava, S. *et al.* The antibacterial lectin RegIIIγ promotes the spatial segregation of microbiota and host in the intestine. *Science (80-.).* (2011) doi:10.1126/science.1209791.

21. Vermeij, W. P. & Backendorf, C. Skin cornification proteins provide global link between ROS detoxification and cell migration during wound healing. *PLoS One* **5**, e11957–e11957 (2010).

22. Fischer, D. F., Gibbs, S., van De Putte, P. & Backendorf, C. Interdependent transcription control elements regulate the expression of the SPRR2A gene during keratinocyte terminal differentiation. *Mol. Cell. Biol.* **16**, 5365–5374 (1996).

23. MW, S., DF, F., E, de M., P, van de P. & C, B. AP-1 and ets transcription factors regulate the expression of the human SPRR1A keratinocyte terminal differentiation marker. *J. Biol. Chem.* **273**, 24683–24692 (1998).

24. Scocchi, M., Tossi, A. & Gennaro, R. Proline-rich antimicrobial peptides: Converging to a non-lytic mechanism of action. *Cellular and Molecular Life Sciences* (2011) doi:10.1007/s00018-011-0721-7.

727 25. Stotz, H. U., Thomson, J. G. & Wang, Y. Plant defensins: defense,
728 development and application. *Plant Signal. Behav.* **4**, 1010–1012 (2009).

729 26. Hu Zehan, Zhang Chenlu….H. L. V. Small proline rich protein 2A is a
730 bactericidal protein that defends the intestinal barrier during helminth infection.
731 (Accepted) *Science (80-.).* (2021).

732 27. Grice, E. A. *et al.* A diversity profile of the human skin microbiota. *Genome*
733 *Res.* (2008) doi:10.1101/gr.075549.107.

734 28. Demetris, A. J. *et al.* Small proline-rich proteins (SPRR) function as SH3
735 domain ligands, increase resistance to injury and are associated with epithelial-
736 mesenchymal transition (EMT) in cholangiocytes. *J. Hepatol.* (2008)
737 doi:10.1016/j.jhep.2007.09.019.

738 29. Chen, Y. E., Fischbach, M. A. & Belkaid, Y. Skin microbiota-host interactions.
739 *Nat. Publ. Gr.* (2018) doi:10.1038/nature25177.

740 30. Lovászi, M., Szegedi, A., Zouboulis, C. C. & Törőcsik, D. Sebaceous-
741 immunobiology is orchestrated by sebum lipids. *Dermatoendocrinol.* **9**,
742 e1375636 (2017).

743 31. Malik, E., Dennison, S. R., Harris, F. & Phoenix, D. A. pH Dependent
744 Antimicrobial Peptides and Proteins, Their Mechanisms of Action and
745 Potential as Therapeutic Agents. *Pharmaceuticals* **9**, (2016).

746 32. Hooper, L. V. *et al.* Molecular Analysis of Commensal Host-Microbial
747 Relationships in the Intestine. *Science (80-.).* **291**, 881–884 (2001).

748 33. Liu, H. *et al.* Staphylococcus aureus Epicutaneous Exposure Drives Skin
749 Inflammation via IL-36-Mediated T Cell Responses. *Cell Host Microbe* **22**,
750 653-666.e5 (2017).

751

Figure 1

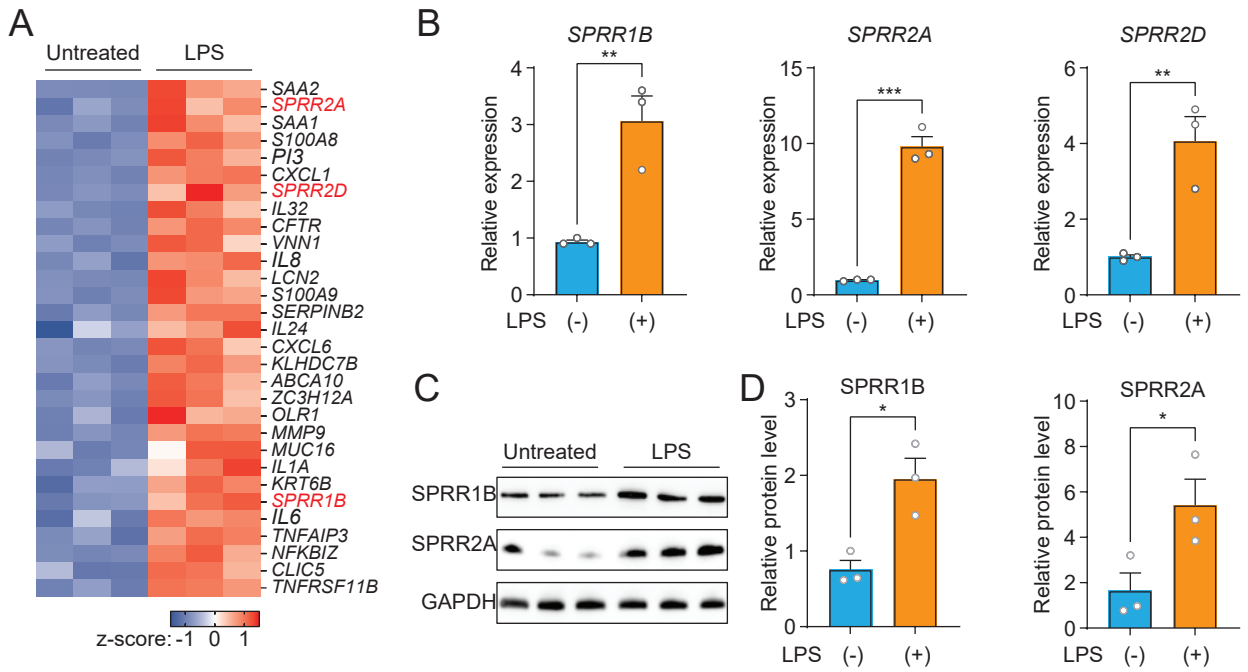

Fig. 1. The expression of *SPRR* family genes are up-regulated by lipopolysaccharide (LPS) in human sebaceous gland cells. (A) Schematic of facial skin derived immortalized human SZ95 sebaceous gland cells treated with LPS for RNA sequencing. (B) Volcano plot with significantly up-regulated genes (fold change>1.4 and adjusted *p* value<0.01) highlighted in red (up regulated in LPS treated). (C) Heat map of significantly up-regulated genes, represented as Z-scored RPKM (reads per kilo base per million reads). *SPRR1B, SPRR2A* and *SPRR2D* are highlighted in red. (D) Reverse transcription-quantitative polymerase chain reaction (RT-qPCR) analysis of *SPRR1B, SPRR2A* and *SPRR2D* transcript in the vehicle and LPS treated human SZ95 sebocytes. (E) Western blot analysis of SPRR1B and SPRR2A was performed on vehicle or LPS treated SZ95 cells. GAPDH was used as the loading control. (F) Quantification of Western blot in (E). Means ± SEM are plotted, **P*<0.05, ***P*<0.01, ****P*<0.001 was determined by unpaired t-test.

Figure 2

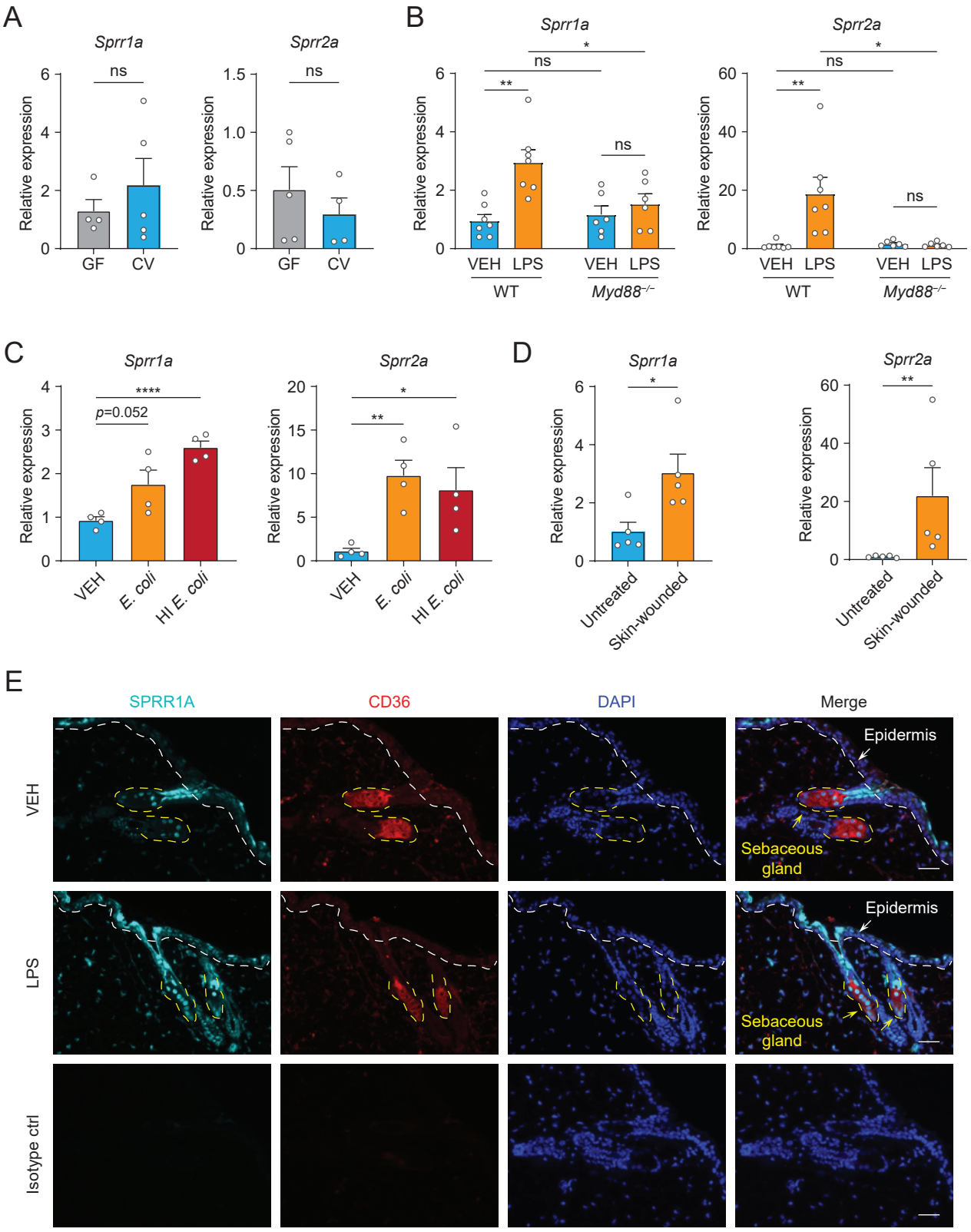
A
Sprr1a
Sprr2a
Relative expression
ns
GF
CV
B
Sprr1a
Sprr2a
ns
*
**
VEH
LPS
WT
Myd88-/-
C
Sprr1a
Sprr2a
****
p=0.052
*
**
VEH
E. coli
HI E. coli
D
Sprr1a
Sprr2a
Untreated
Skin-wounded
E
SPRR1A
CD36
DAPI
Merge
VEH
LPS
Isotype ctrl
Epidermis
Sebaceous gland

Fig. 2. The expression of *SPRR* family genes are up regulated by LPS in mice. (A-D) qRT-PCR analysis of *Sprr1a* and *Sprr2a* gene expression in mouse dorsal skin tissue. (A) Germ-free mice (GF) compared to conventionally raised mice (CV). (B) PBS treated mouse skin compared to LPS intradermal injection mouse skin in WT or MYD88$^{-/-}$ mouse. (C) Mouse intradermally-injected by vehicle (PBS), *E.coli* or heat-inactivated (HI) E.coli. (D) Untreated mouse skin compared to wounded skin abraded in a crosshatch pattern by a 15-blade scalpel. Means ± SEM are plotted. *P < 0.05; **P < 0.01; ****P < 0.0001ns, not significant by unpaired t test. (E) Immunofluorescence staining of SPRR1A expression in mice skin. CD36 was used as marker of sebocyte cells. Nuclei are stained with DAPI (Blue). Epidermis and sebaceous gland indicated with an arrow. White dashed line separates the epidermis and dermis. Yellow dashed line indicates the outline of SG. Scale bar, 50 μm.

Figure 3

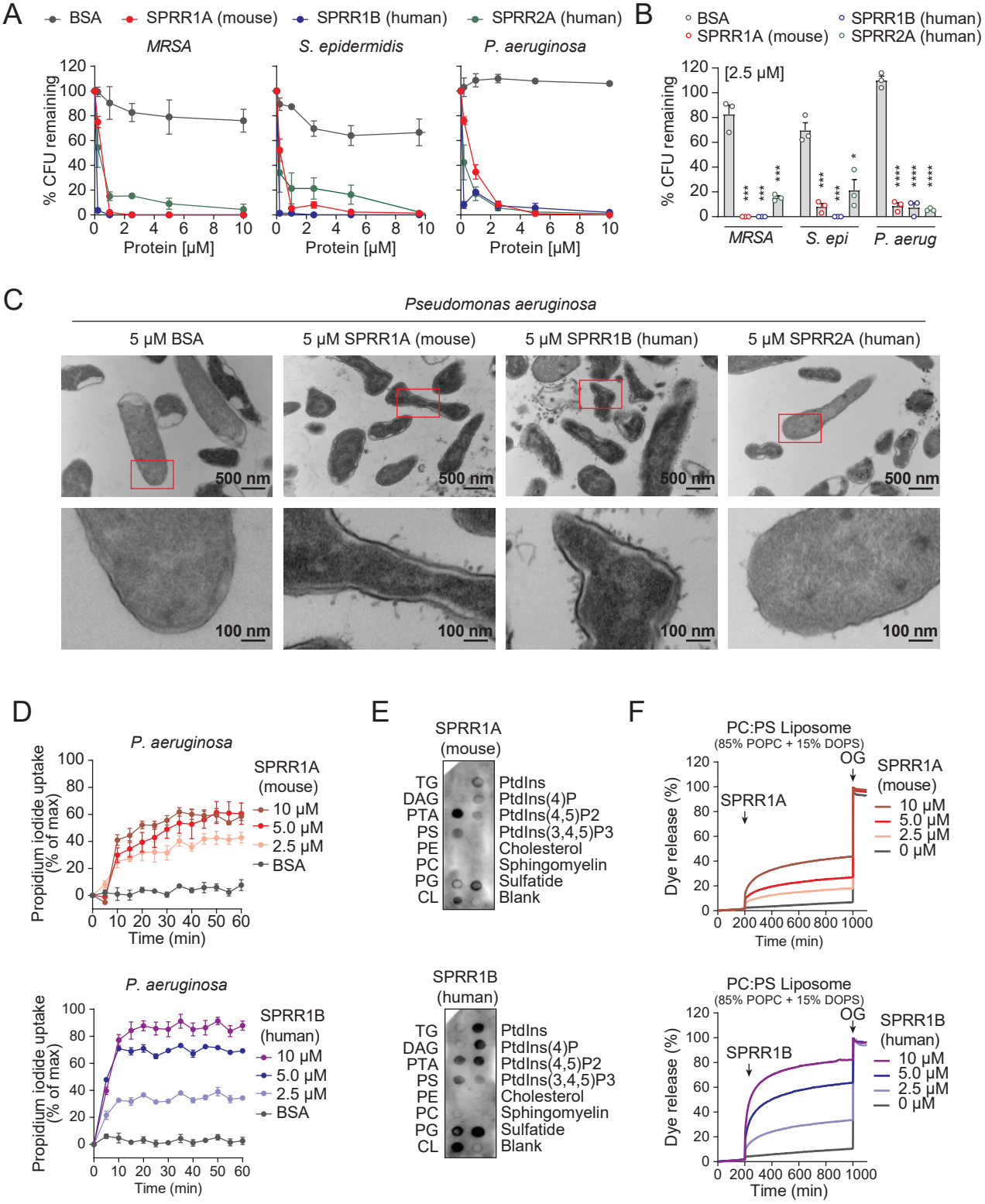
A
BSA
SPRR1A (mouse)
SPRR1B (human)
SPRR2A (human)
MRSA
S. epidermidis
P. aeruginosa
% CFU remaining
Protein [μM]
B
BSA
SPRR1A (mouse)
SPRR1B (human)
SPRR2A (human)
[2.5 μM]
% CFU remaining
MRSA
S. epi
P. aerug
C
Pseudomonas aeruginosa
5 μM BSA
5 μM SPRR1A (mouse)
5 μM SPRR1B (human)
5 μM SPRR2A (human)
500 nm
100 nm
D
P. aeruginosa
Propidium iodide uptake (% of max)
Time (min)
SPRR1A (mouse)
10 μM
5.0 μM
2.5 μM
BSA
SPRR1B (human)
E
SPRR1A (mouse)
SPRR1B (human)
TG
DAG
PTA
PS
PE
PC
PG
CL
PtdIns
PtdIns(4)P
PtdIns(4,5)P2
PtdIns(3,4,5)P3
Cholesterol
Sphingomyelin
Sulfatide
Blank
F
PC:PS Liposome
(85% POPC + 15% DOPS)
OG
SPRR1A
SPRR1B
Dye release (%)
Time (min)
0 μM

Fig. 3. SPRR family proteins exert bactericidal activity against various skin commensal and pathogenic bacteria by membrane disruption. (A) Increasing concentrations of purified recombinant SPRR proteins were added to mid-logarithmic phase *MRSA*, *S. epidermidis*, *P.aeruginosa* for 2 hours and surviving bacteria were quantified by dilution plating. (B) 2.5 μM of SPRR proteins was added to midlogarithmic phase bacteria for 2 hours and surviving bacteria were quantified by dilution plating. Remaining Colony forming units (CFUs) are expressed as a percentage of untreated bacteria control. (C) Transmission electron microscopy of *P. aeruginosa* after incubation with 5 μM purified recombinant SPRR proteins. BSA was used as negative control. Examples of cell surface damage and cytoplasmic leakage are indicated with red rectangular box. Upper scale bars, 500 nm. Lower scale bars, 100 nm. (D) Propidium iodide (PI) uptake by *P. aeruginosa* in the presence of increasing concentrations of mouse SPRR1A and human SPRR1B protein. (E) Membranes displaying various lipids were incubated with 1μg/mL SPRR proteins, and detected with specific antibody. (F) Carboxyfluorescein (CF)-loaded liposomes were treated with increasing concentrations of mouse SPRR1A and human SPRR1B protein, and dye efflux was monitored over time and was expressed as a percentage of total efflux in the presence of the detergent octyl glucoside (OG). All assays were performed in triplicate. Means ± SEM are plotted. *$P < 0.05$; ***$P < 0.001$; ****$P < 0.0001$; ns, not significant by two-tailed t-test.

Figure 4

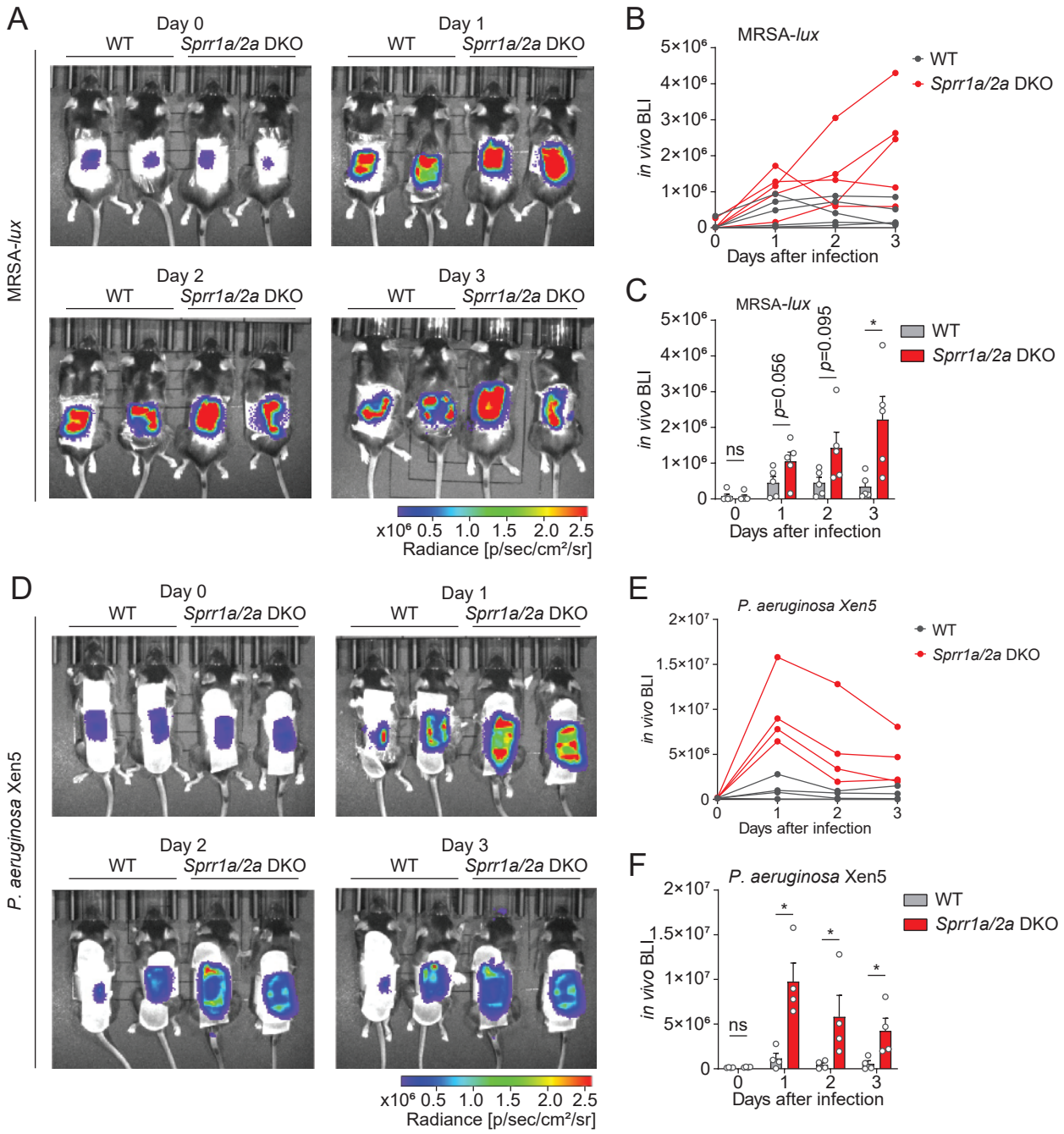

Fig. 4. SPRR family proteins protect against skin MRSA and *P. aerugonisa* infection. (A-C) WT and *Sprr1a*$^{-/-}$;*Sprr2a*$^{-/-}$ mice were epicutaneously challenged with MRSA (1 x 10^6 CFU) on the shaved dorsal skin for 3 consecutive days. (A) Representative *in vivo* bioluminescent imaging (BLI) photographs from Day 0 to Day 3. Quantification of MRSA total flux (photons/s) for each mouse (B) or plotted as Means ± SEM (C). (D-F) WT and *Sprr1a*$^{-/-}$;*Sprr2a*$^{-/-}$ mice were superficially abraded in a crosshatch pattern by a 15-blade scalpel to introduce skin wounding. One day post crosshatch wounding, WT and *Sprr1a*$^{-/-}$;*Sprr2a*$^{-/-}$mice were topically applied with 1 x 10^6 CFU *P. aerugonisa* on the back skin for 3 days. (D) Representative in vivo bioluminescent imaging (BLI) signals from Day 0 to Day 3. Quantification of *P. aerugonisa* total flux (photons/s) for each mouse (E) or plotted as Means ± SEM (F). *$p < 0.05$, ns, not significant by unpaired t-test.

figure 1

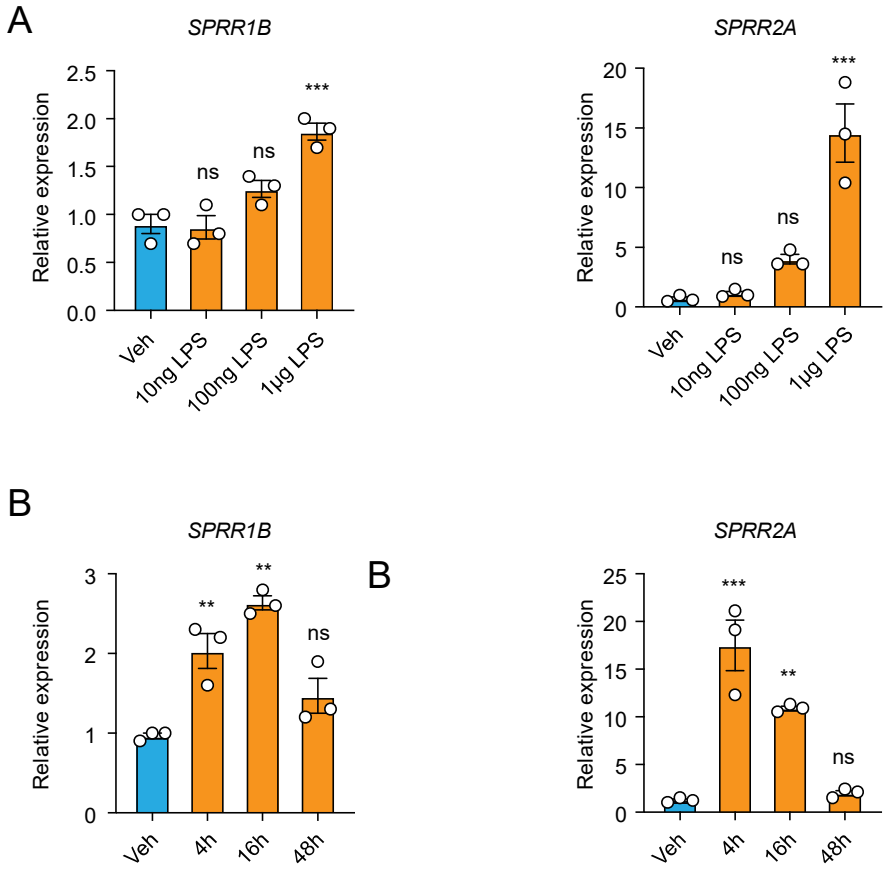

fig. S1. Dose response and time course analysis of LPS treatment on human sebocyte cells. qRT-PCR analysis of *SPRR1B and SPRR2A* transcript in the vehicle and various LPS treated human SZ95 sebocytes. (A) SZ95 sebocyte cells were treated with different concentration of LPS for 16 hours. (B) SZ95 cell were treated with 1 μg/mL LPS for different length of time. Means ± SEM are plotted. **P < 0.01; ***P < 0.001;ns, not significant by unpaired t-test.

figure 2

A

TLR Ligands	Targets	Description
Pam3CSK4	TLR1/2	Tripalmitoylated lipopeptide that mimics the bacterial lipoprotein
HKLM	TLR2	Heat-killed *Listeria monocytogenes*
Poly(I:C) HMW	TLR3	Double-strand RNA (1.5-8kb)
Poly(I:C) LMW	TLR3	Double-strand RNA (0.2-1kb)
LPS	TLR4	Lipopolysaccharide
Flagellin	TLR5	Component of the bacterial flagellar filament
FSL-1	TLR6/2	Lipopeptide that mimics the lipoprotein LP44 of *Mycoplasma salivarium*
Imiquimod	TLR7	An imidazoquinoline amine analog to guanosine

B

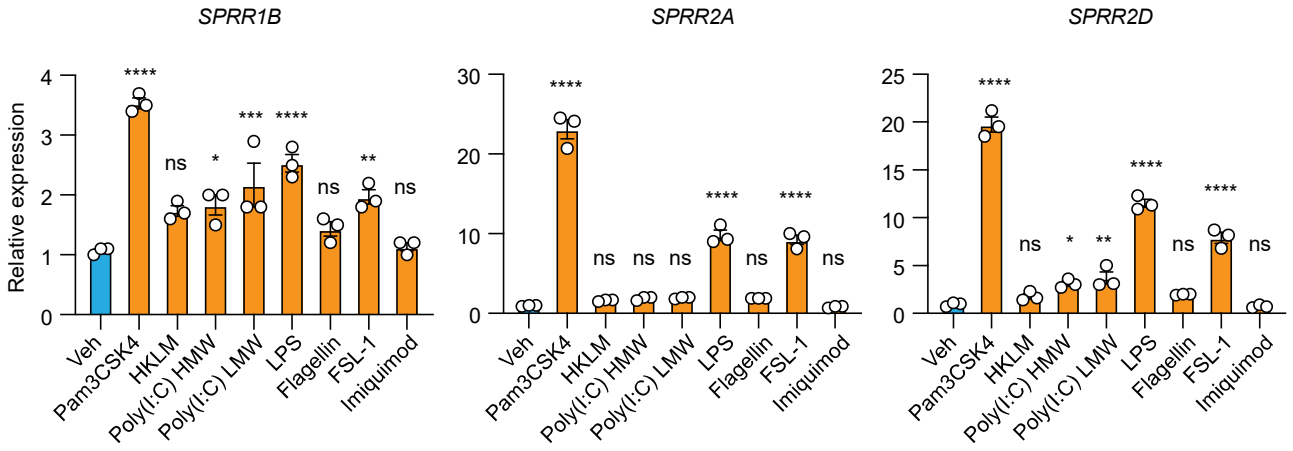

fig. S2. The expression of SPRR family genes are up regulated by TLR2 and TLR4 agonists in human sebaceous gland cells. (A) A list of different TLR agonists. (B) qRT-PCR analysis of *SPRR* family genes expression in the vehicle and various TLR agonists treated SZ95 cells. Means ± SEM are plotted. *P < 0.05; **P < 0.01; ***P < 0.001; ****P < 0.0001; ns, not significant by one-way ANOVAs.

figure 3

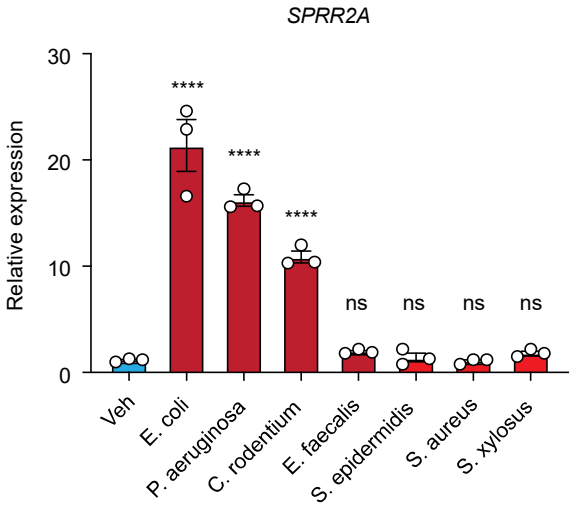

fig. S3. Gram-negative bacteria can trigger *Sprr2a* gene expression in human sebaceous gland cells. qRT-PCR analysis of *Sprr2a* transcript in the vehicle and various heat inactivated bacteria treated human SZ95 sebocyte cells. Means ± SEM are plotted. ****P < 0.0001; ns, not significant by one-way ANOVAs.

figure 4

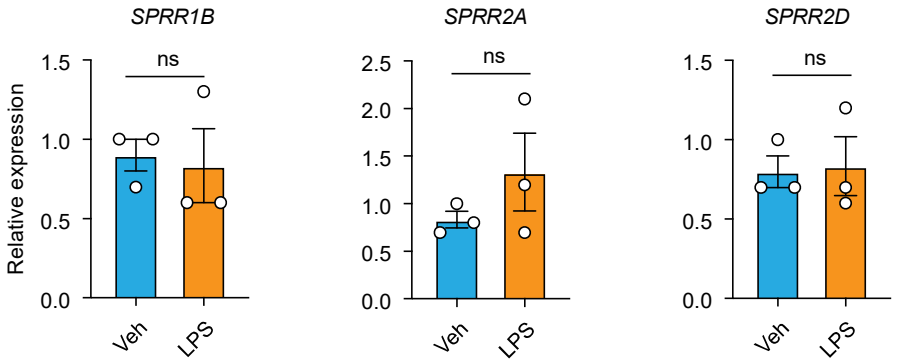

fig. S4. LPS cannot induce the expression of *SPRR* family genes in human keratinocyte cells. hTERT immortalized human keratinocyte cells were treated with LPS for 16 hours. qRT-PCR analysis of *SPRR1B, SPRR2A* and *SPRR2D* transcript in the vehicle and LPS treated human hTERT keratinocytes. Means ± SEM are plotted. ns, not significant by unpaired t-test.

figure 5

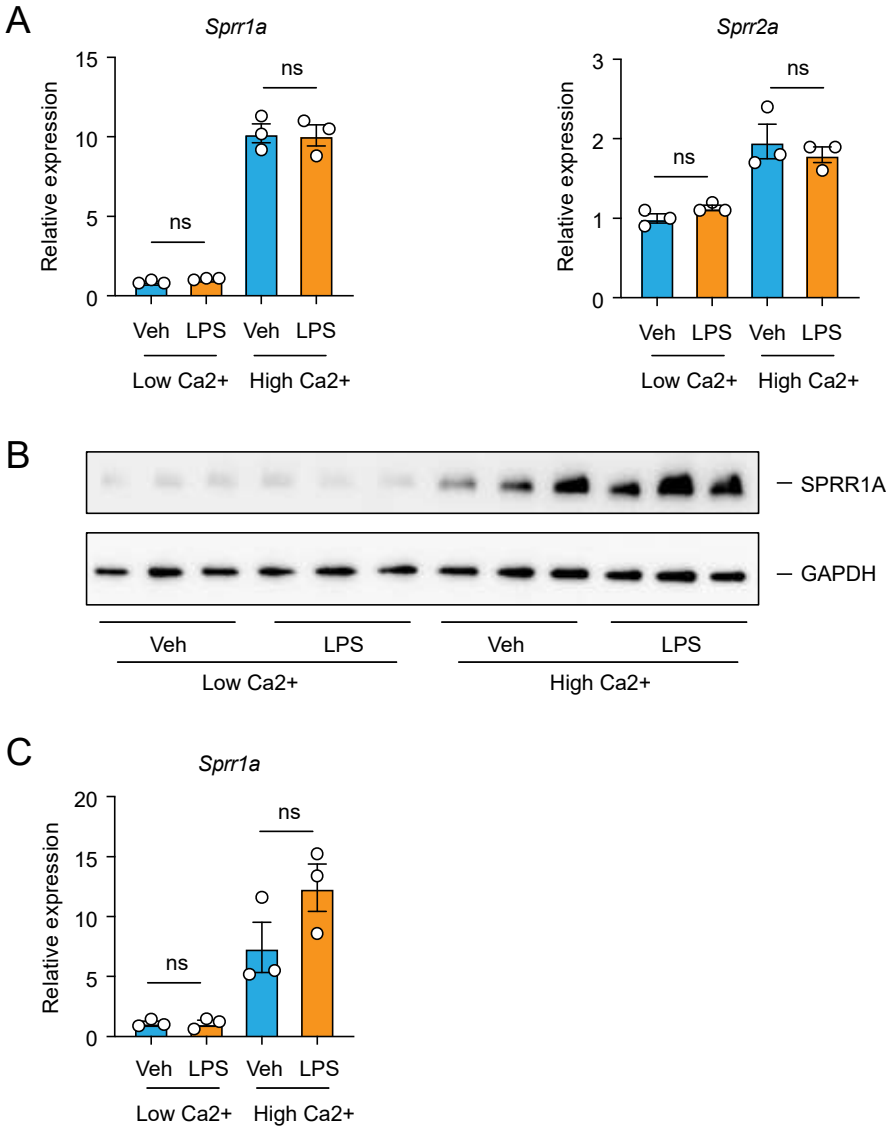

fig. S5. LPS cannot trigger the expression of *Sprr* family genes in primary mouse keratinocytes. Primary mouse keratinocytes were isolated from 3-5 days old neonatal mice through dispase digestion. With 0.05 mM $CaCl_2$ (Low Ca^{2+}), keratinocytes can proliferate but won't differentiate into a stratified layer. Under 1 mM $CaCl_2$ (High Ca^{2+}) condition, keratinocytes will initiate differentiation process. (A) qRT-PCR analysis of *Sprr1a* and *Sprr2a* transcript in the vehicle and LPS treated primary mouse keratinocyte cells cultured under Low Ca^{2+} or High Ca^{2+} condition. (B) Western blot analysis of SPRR1A protein was performed on vehicle or LPS treated primary mouse keratinocytes under both Low Ca^{2+} and High Ca^{2+} condition. (C) Quantification of the Western blot in (B). Means ± SEM are plotted. *$P < 0.05$; ***$P < 0.001$ by unpaired t-test.

figure 6

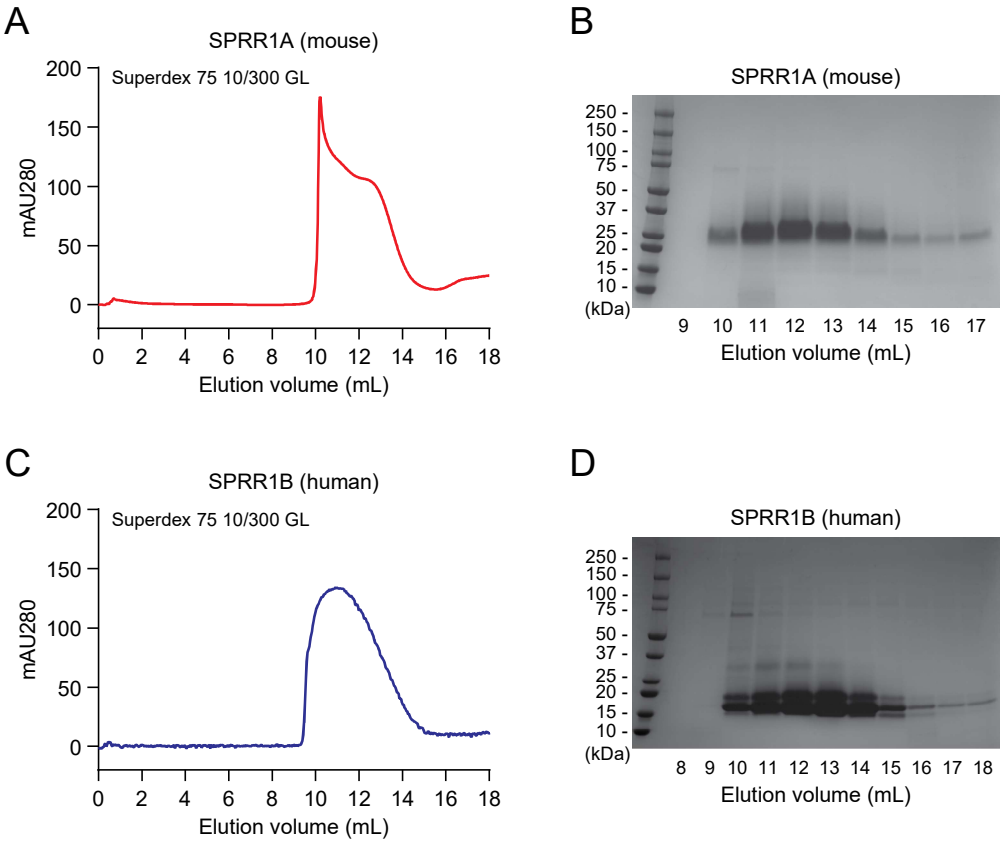

fig. S6. Recombinant expression and purification of SPRR proteins. (A and C) Recombinant mouse SPRR1A protein (A) and human SPRR1B protein (C) was expressed using a baculovirus expression system and purified by size-exclusion chromatography (Superdex 75 10/300 GL) [26]. (B and D) Fractions from (A) and (C) were visualized by Coomassie blue staining following SDS-polyacrylamide gel electrophoresis (SDS-PAGE).

figure 7

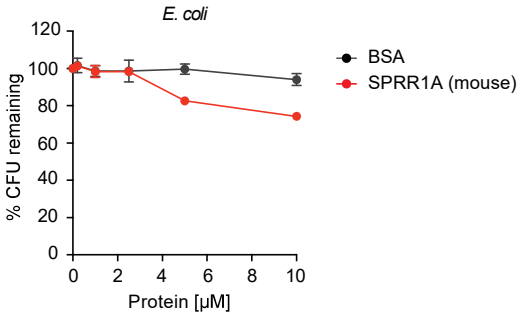

fig. S7. SPRR1A protein was resistant to Gram-negative bacteria *Escherichia coli*. Increasing concentrations of purified recombinant mouse SPRR1A protein was added to mid-logarithmic phase *Escherichia coli* for 2 hours and surviving bacteria were quantified by dilution plating. Remaining Colony forming units (CFUs) are expressed as a percentage of untreated bacteria control. BSA was used as negative control. Means ± SEM are plotted.

figure 8

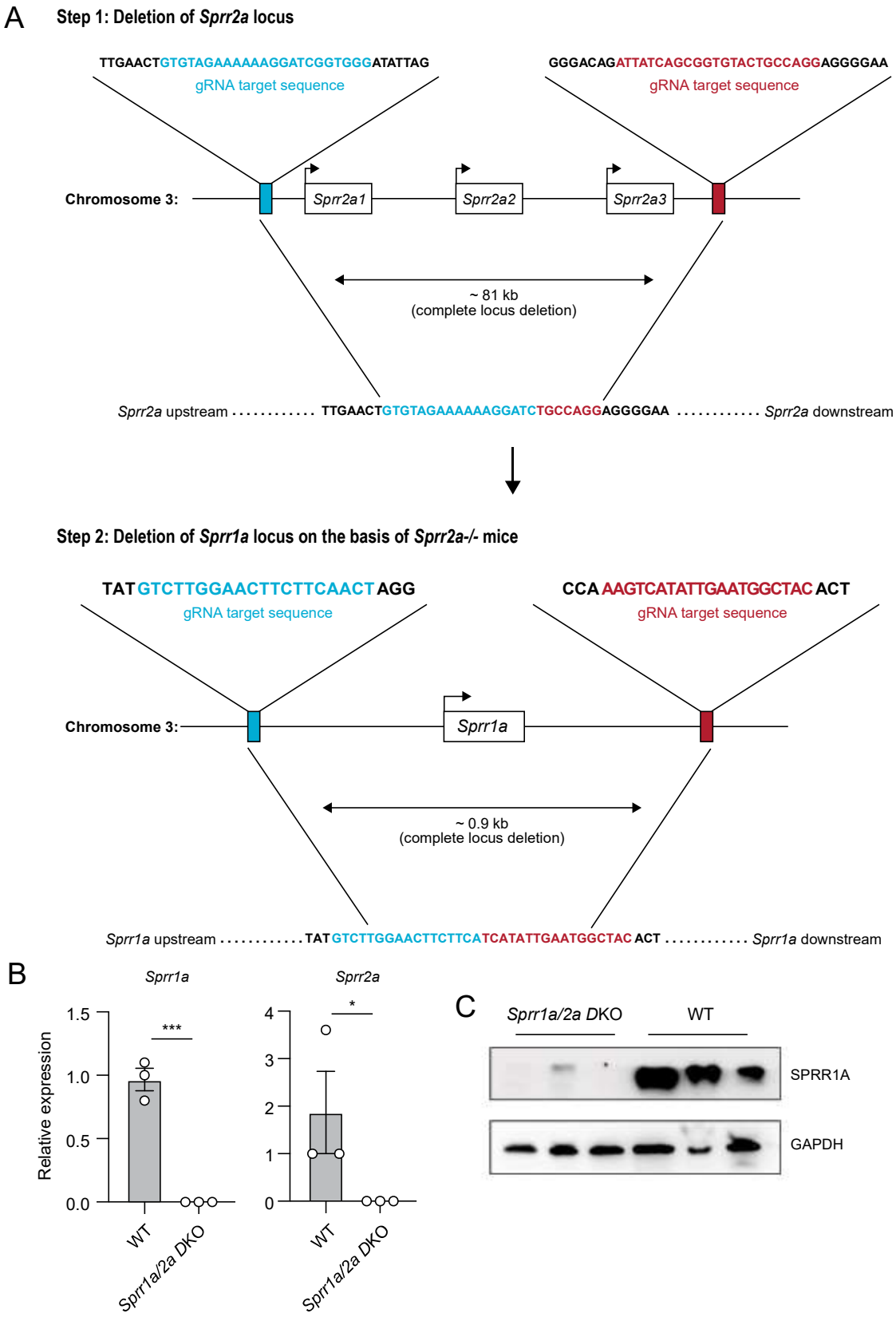

fig. S8. Generation and validation of *Sprr1a*$^{-/-}$;*Sprr2a*$^{-/-}$mice by CRISPR/Cas9 genomic targeting. (A) Schematic diagram of two-step strategy using CRISPR/Cas9-mediated gene targeting to delete the entire *Sprr2a* and *Sprr1a* locus. (B) qRT-PCR analysis of *Sprr1a* and *Sprr2a* expression in the skin of WT and *Sprr1a*$^{-/-}$;*Sprr2a*$^{-/-}$ mice. Values were normalized to *Gapdh* expression. Means ± SEM are plotted. *P < 0.05; ***P < 0.001 by unpaired t-test. (C) Western blot analysis of SPRR1A protein in the skin of WT and *Sprr1a*$^{-/-}$;*Sprr2a*$^{-/-}$mice. GAPDH was used as the loading control.

figure 9

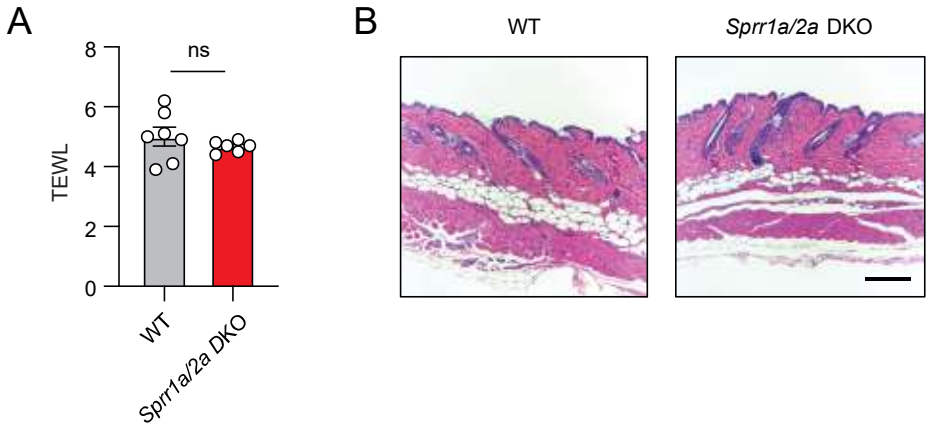

fig. S9. *Sprr1a*$^{-/-}$*;Sprr2a*$^{-/-}$ mice does not show signs of inflammation or impaired skin barrier. (A) Transepidermal water loss (TEWL) of WT and *Sprr1a*$^{-/-}$*;Sprr2a*$^{-/-}$mice skin was analyzed. Means ± SEM is plotted, ns, not significant by unpaired t test. (B) Representative H&E staining of mouse skin from WT and *Sprr1a*$^{-/-}$*;Sprr2a*$^{-/-}$. Scale bar, 200 µm.